Alexandria Engineering Journal (2016) 55, 2647–2654

Alexandria University

Alexandria Engineering Journal

www.elsevier.com/locate/aej
www.sciencedirect.com

ORIGINAL ARTICLE

Evaluating interfacial shear stresses in composite hollowcore slabs using analytical solution

Aiham Adawi [a], **Maged A. Youssef** [a], **Mohamed E. Meshaly** [b,*]

[a] *Department of Civil and Environmental Engineering, Western University, London, Ontario N6A 5B9, Canada*
[b] *Department of Structural Engineering, Alexandria University, Alexandria, Egypt*

Received 1 June 2016; revised 22 June 2016; accepted 2 July 2016
Available online 21 July 2016

KEYWORDS

Composite hollowcore slabs;
Interfacial shear stress;
Full-scale tests;
Analytical modeling;
Finite element modeling

Abstract Analytical evaluation of the interfacial shear stresses for composite hollowcore slabs with concrete topping is rare in the literature. Adawi et al. (2014) estimated the interfacial shear stiffness coefficient (k_s) that governs the behavior of the interface between hollowcore slabs and the concrete topping using push-off tests. This parameter is utilized in this paper to provide closed form solutions for the differential equations governing the behavior of simply supported composite hollowcore slabs. An analytical solution based on the deformation compatibility of the composite section and elastic beam theory, is developed to evaluate the shear stresses along the interface. Linear finite element modeling of the full-scale tests presented in Adawi et al. (2015) is also conducted to validate the developed analytical solution. The proposed analytical solution was found to be adequate in estimating the magnitude of horizontal shear stress in the studied composite hollowcore slabs.

1. Introduction

Hollowcore slabs are precast/prestressed structural concrete elements that are commonly used in residential and commercial buildings. They have the advantage of higher quality, ease of installation, and reduced construction times compared with cast-in-situ slabs. Floor surface irregularities may rise from the differential camber between adjacent slabs. Thus, to achieve a flat surface finish, a 50 mm concrete topping is commonly cast on top of the hollowcore slabs. Design engineers tend to consider the composite action between the concrete topping and the slabs to increase the load carrying capacity of the floor. This requires roughening of the surface of the hollowcore slab to an amplitude of 6.35 mm or 5.00 mm according to [1] and [6], respectively. Some design engineers require the use of bonding agents in addition to the roughening mentioned in the design standards, which induce additional costs that hollowcore slab manufacturers are keen to avoid. There is a general consensus among manufacturers that the bond between hollowcore slabs with machine-cast surface and topping concrete is sufficient to develop adequate composite action. This emphasizes the need for more studies that shed light on the adequacy of composite action in hollowcore slabs with machine-cast surface.

Most of the literature on composite action of slabs is related to composite steel beams [5,10,7,8] where the concrete topping is attached to the top flange of the steel beam using shear connectors (shear studs). Salari et al. [13] and [12] modeled the shear connectors using spring element and their stiffnesses were evaluated through push-off tests similar to

* Corresponding author.
Peer review under responsibility of Faculty of Engineering, Alexandria University.

http://dx.doi.org/10.1016/j.aej.2016.07.001

Nomenclature

a	distance from edge of hollowcore slab to edge of concrete topping
A_t	cross-sectional area of concrete topping
b	distance from edge of hollowcore slab to the applied concentrated load (P)
b_t	width of concrete topping
E_{hc}	young's modulus of concrete for hollowcore slab
E_t	young's modulus of concrete for concrete topping
I_{hc}	moment of inertia of hollowcore slab
I_t	moment of inertia of concrete topping
K	general interfacial shear stiffness
k_s	interfacial shear stiffness
L	hollowcore slabs length
L_t	length of concrete topping
M_{hc}	internal moment in hollowcore slab
M_t	internal moment in concrete topping
M_T	total external moment
N	normal force
P	concentrated applied load
P_y	yielding load
Q	distributed load on composite slab
u_{hc}	displacement of hollowcore slab at the interface layer
u_t	displacement of concrete topping at the interface layer
V_{hc}	vertical shear force in hollowcore slab
V_T	total external shear
V_t	vertical shear force in concrete topping
Y_{hc}	distance from the interface layer to hollowcore slab's mid-depth
Y_t	distance from the interface layer to the middle of concrete topping
σ	interfacial peel stress
τ	interfacial shear stress
τ_{avg}	average interfacial stress using North American design standards methods
ε_{hc}	strain in hollowcore slab at the interface layer
ε_t	strain in concrete topping at the interface layer

the test conducted by Ollgard et al. [11]. In another type of composite steel beams an adhesive compound, such as epoxy, is utilized to attach the concrete topping to the steel beam instead of shear studs. Luo et al. [9] conducted push-off tests on the bonded composite steel samples to evaluate the shear behavior of the adhesive. The interface between the hollowcore slab and the concrete topping in a typical composite slab does not contain studs or adhesive layers and therefore cannot be addressed using such research studies. However, the push-off tests used by those researchers can be used to estimate the interface shear strength for composite hollowcore slabs.

Steel plates or fiber-reinforced polymer laminates are commonly used to increase the flexural load capacity of concrete beams. These plates are attached to the soffit of the beam using a bonding agent and/or mechanical anchors. Ideally, the ultimate flexural capacity of the retrofitted beam is supposed to be reached prior to delamination of the plate.

Vilnay [15] presented an analytical method to estimate the shear stresses between a reinforced concrete beam and a steel plate bonded to its soffit. The method does not account for the axial deformations of the beam, the bending deformations of the plate, and the shear deformations of the interface layer. It is only applicable for the case of a point load applied at midspan and assumes zero shear stress under that load.

Smith and Teng [14] proposed an analytical solution to determine the shear stress distributions at the interface. Their approach accounts for the bending deformations of the plate and the axial deformations of the beam. The interfacial shear stress is assumed to be continuous at the point load. This approach can be applied to general load scenarios.

In composite slab systems, the average horizontal shear stress is calculated using the two methods available in the North American design standards [6,1]. The first method utilizes the shear force diagram for calculations and applies only for the case when the concrete topping is poured over the entire slab length. The second method uses the strain compatibility to determine the horizontal shear force in the concrete topping. Both methods assume that the concrete topping is fully bonded to the slab and therefore does not account for the interfacial shear stiffness of the interface. Including the effect of interfacial shear stiffness (k_s) may affect the distribution of the horizontal shear stresses along the interface layer, which needs to be investigated.

Adawi et al. [2] tested four composite hollow-core slabs with concrete topping using push-off tests. The slabs had machine cast finish and lightly roughened surfaces. The slabs were analyzed using linear analytical modeling that provided solutions for the deferential equations governing the equilibrium of the push-off tests. As a result, the shear stiffness of the interface between the hollowcore slabs and the concrete topping was determined for the tested slabs.

Adawi et al. [3] conducted a comprehensive experimental program including sixty-nine pull-off tests, and six push-off and six full-scale tests. Tests were performed on slabs with machine cast and lightly roughened surfaces. The program also included a procedure to evaluate the surface roughness of hollowcore slabs that can be used by manufacturers a quality control measure during production to insure adequate composite action.

In this paper, a brief summary about two composite hollowcore slabs that were tested in full-scale by Adawi et al. [3] is first given. An analytical solution that is based on Smith and Teng [14] approach is then presented. This solution includes the bending and axial deformations of the concrete topping and the hollowcore slab and can be applied to any load case. It also takes into account the effect of the interfacial shear stiffness (k_s) that is neglected in code methods. The interfacial shear stiffness (k_s) is a measure of the resistance of the interface layer to slip deformation. The (k_s) values used in this paper were evaluated using analytical analysis conducted in Adawi et al. [3]. These values may vary between slabs depending on the surface roughness, which can be evaluated using the procedure explained in Adawi et al. [3]. Results of a linear finite element analysis of the full-scale tests are then compared

with the results obtained from the analytical solution for validation.

2. Full-scale tests

Adawi et al. [3] tested two composite hollowcore slabs in full-scale, FMA2-1 and FMB2-2, which were topped with 50 mm concrete. Table 1 summarizes the slab dimensions and properties. The slabs had a machine-cast surface with average surface roughness of 0.311 mm based on the procedure explained in Adawi et al. [3]. This is considerably lower than the 6.35 mm and 5.00 mm intentional-roughness amplitudes required by [6] and ACI 318-08 [1], respectively. The full-scale tests were conducted using the three point bending test setup as shown in Fig. 1.

The span was 2658 mm and the concentrated load was applied at mid-span using a steel spreader beam. The slabs were instrumented with gauges to measure strains in the hollowcore slabs and the concrete topping during the test. Shear displacements were measured using four LVDTs that were distributed symmetrically along the slab. Both slabs showed adequate composite performance up to failure. The predicted failure loads were 262 kN and 382 kN for slabs FMA2-1 and FMB2-2, respectively. Test failure loads were obtained as 253 kN and 410 kN for slabs FMA2-1 and FMB2-2, respectively. Fig. 2 shows the load-deflection curves for both slabs as obtained from the tests. The curves present a typical flexural behavior starting with a linear stiffness up to yielding load followed by a nonlinear segment up to failure.

Slab FMA2-1 had four 13 mm diameter strands while slab FMB2-2 had seven of the same strands. This explains the higher yielding load for slab FMB2-2 and the more ductile behavior of slab FMA1-2. Yielding loads were estimated using the load-deflection curves as 160 kN and 233 kN for slab FMA1-2 and FMB2-2, respectively. Slab FMA2-1 failed in flexural mode by crushing of topping concrete in the vicinity of the load. Flexure-shear failure mode was observed for slab FMB2-2 emphasized by an inclined crack close to the support.

The visual inspection performed during the full-scale test showed no signs of delamination of the concrete toping up to failure loads. This observation along with the comparable predicted versus test failure loads suggests an adequate composite action for both slabs up to failure.

3. Analytical modeling

Smith and Teng [14] proposed an analytical solution to determine the shear stress distribution in the adhesive layer connecting Fiber-Reinforced Plastics (FRP) or steel plates to the soffit of beams. The same approach is used in this section, however the derivation is modified to accommodate two main differences: (1) the concrete topping is located on top of slab and not at the soffit side and (2) there is no adhesive to connect the concrete topping to the hollowcore slab; thus, the thickness of the interface layer is equal to zero. The approach accounts for the bending deformations of the plate and the axial deformations of the beam. The shear stiffness (k_s) obtained from Adawi et al. [2] will be used here to characterize the strength properties of the interface between the concrete topping and the hollowcore slab.

This section shows the derivation and solution of the differential equations governing the equilibrium of the full-scale

Table 1 Slab specimen properties.

Slab label	Length (mm)	Width (mm)	Thickness (mm)	Surface roughness (mm)	Strands pattern # - diameter (mm)	Concrete compressive strength f'_c, MPa
FMA2-1	3658	1220	203	0.325	4–13	50
FMB2-2	3658	1220	203	0.297	7–13	58

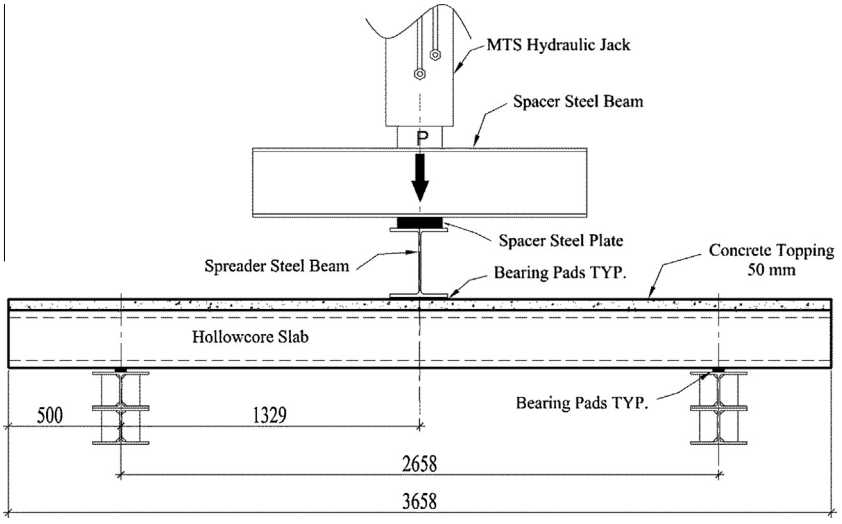

Figure 1 Full-scale test setup, Adawi et al. [3].

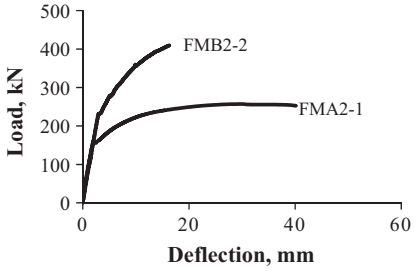

Figure 2 Load-deflection test results.

tests to determine the shear stress distribution along the interface between the hollowcore slabs and the concrete topping. The applied load used in the analytical solutions is not the failure load from the full-scale tests but it is the yield load (P_y) at which the response turns into the nonlinear stage. Thus, the analytical solutions are derived based on the elastic beam theory, which does not include the effect of cracking.

Fig. 3 shows the forces acting on a segment (dx) of a simply supported composite hollowcore slab that is loaded with a uniformly distributed load (Q). The peel stress (σ) is shown in the figure for illustration but will not be studied in the scope of this paper.

The interface has a thickness zero. The value [$N \times (y_{hc} + y_t)$] represents the moment component resisted by the composite section. The moment and the vertical shear resisted by the hollowcore slab and the concrete topping are (M_{hc}, V_{hc}) and (M_t, V_t), respectively.

From the equilibrium of the forces and moments that are shown in Fig. 3,

$$\frac{dN}{dx} = b_t\tau \tag{1}$$

$$\frac{dM_{hc}}{dx} = V_{hc} - b_t\tau y_{hc} \tag{2}$$

$$\frac{dM_t}{dx} = V_t - b_t\tau y_t \tag{3}$$

$$dN = K(u_{hc} - u_t) \tag{4}$$

where (K) is the general shear stiffness of the interface in N/mm and (u_{hc}–u_t) is the relative displacement between the top of the hollowcore slab (u_{hc}) and the bottom of the concrete topping (u_t).

By dividing Eq. (4) by ($b_t dx$) where b is the width of the concrete topping, differentiating with respect to (x), and noting that the total strain at the bottom of the concrete topping is $\varepsilon_t = du_t/dx$ and the total strain at the top of the hollowcore slab is $\varepsilon_{hc} = du_{hc}/dx$, the following equation can be reached.

$$\frac{d\tau}{dx} = k_s(\varepsilon_{hc} - \varepsilon_t) \tag{5}$$

where (k_s) is the interfacial shear stiffness in (N/mm)/mm^2.

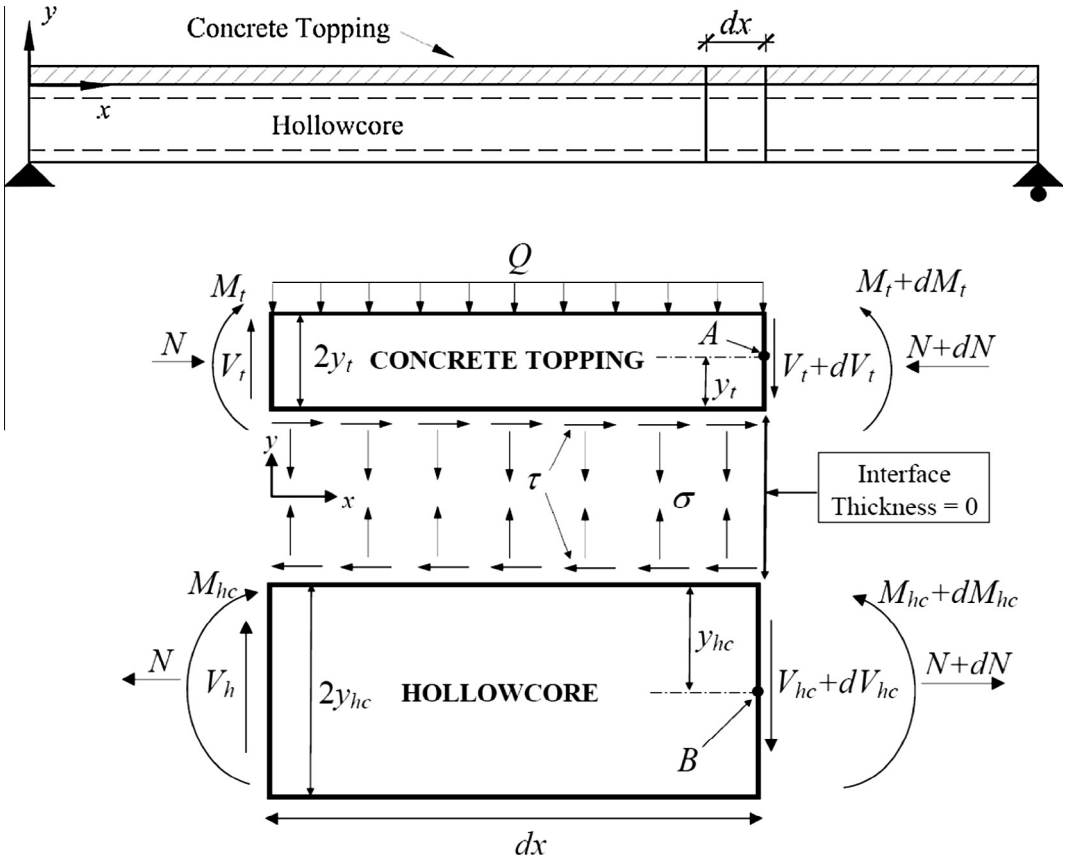

Figure 3 Equilibrium forces of segment (dx).

ε_t and ε_{hc} can be determined based on the moments and normal forces in the hollowcore slabs and the concrete topping as described by Eqs. (6) and (7).

$$\varepsilon_t = \frac{M_t y_t}{E_t I_t} - \frac{N}{E_t A_t} \tag{6}$$

$$\varepsilon_{hc} = \frac{-M_{hc} y_{hc}}{E_{hc} I_{hc}} + \frac{N}{E_{hc} A_{hc}} \tag{7}$$

In the following sections, the differential equations governing the shear stresses acting on the element that is shown in Fig. 3 are first derived using the proposed method. They are then solved for the case of an applied point load at mid-span to obtain the shear stress distribution along the interface between a hollowcore slab and the concrete topping.

3.1. Interfacial shear stress (τ)

The proposed solution follows Smith and Teng's approach (2001). It includes the effect of bending deformations of the concrete topping. The ratio between the moment resisted by the slab and that resisted by the topping can be based on their relative rigidity.

$$M_{hc} = \frac{E_{hc} I_{hc}}{E_t I_t} M_t = R M_t \tag{8}$$

The moment equilibrium of the infinitesimal segment implies that:

$$M_T = M_{hc} + M_t + [N(y_t + y_{hc})] \tag{9}$$

Solving Eqs. (8) and (9) for (M_{hc}) and (M_t) and differentiating with respect to (x) will lead to the following:

$$\frac{dM_{hc}}{dx} = \frac{R}{R+1}[V_T - b_t \tau (y_t + y_{hc})] \tag{10}$$

$$\frac{dM_t}{dx} = \frac{1}{R+1}[V_T - b_t \tau (y_t + y_{hc})] \tag{11}$$

where (M_T) and (V_T) are the total moment and total vertical shear.

By differentiating Eq. (5) with respect to (x) and substituting with Eqs. (6), (7), (10) and (11), the second order differential equation that governs the interfacial shear stress can be obtained.

$$\frac{d^2\tau}{dx^2} = k_s b_t \tau \left[\frac{(y_{hc}+y_t)^2}{E_{hc}I_{hc}+E_tI_t} + \frac{1}{E_{hc}A_{hc}} + \frac{1}{E_tA_t}\right] - k_s V_T \left[\frac{(y_{hc}+y_t)}{E_{hc}I_{hc}+E_tI_t}\right] \tag{12}$$

The general solution of Eq. (12) is given by the following:

$$\tau = B_1 \cosh(\lambda x) + B_2 \sinh(\lambda x) + m_1 V_T \tag{13}$$

where $\lambda^2 = k_s b_t \left[\frac{(y_{hc}+y_t)^2}{E_{hc}I_{hc}+E_tI_t} + \frac{1}{E_{hc}A_{hc}} + \frac{1}{E_tA_t}\right]$ and $m_1 = \frac{k_s}{\lambda^2}\left[\frac{(y_{hc}+y_t)}{E_{hc}I_{hc}+E_tI_t}\right]$

The constants are evaluated below using the boundary conditions for the general case of a hollowcore slab with partial concrete topping. All potential locations of the load (P) relative to the concrete topping are considered as shown in Fig. 4.

Case 1: Load acting on the topping slab ($a < b$), Fig. 4(a):

The boundary conditions for this case are as follows:

at $x = 0, M_T = M_{hc} = Pa\left(1 - \frac{b}{L}\right)$

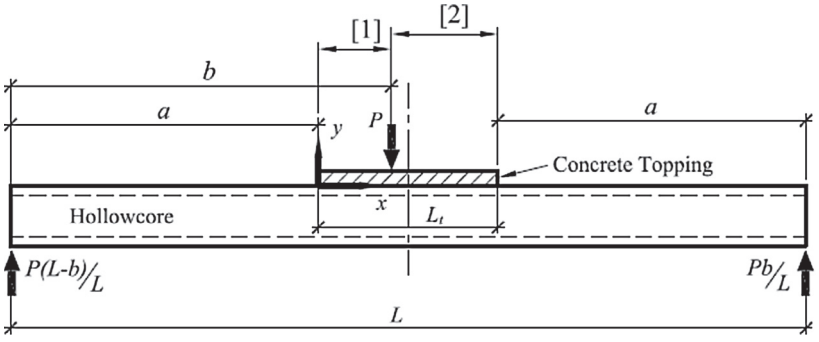

(a) $a < b$

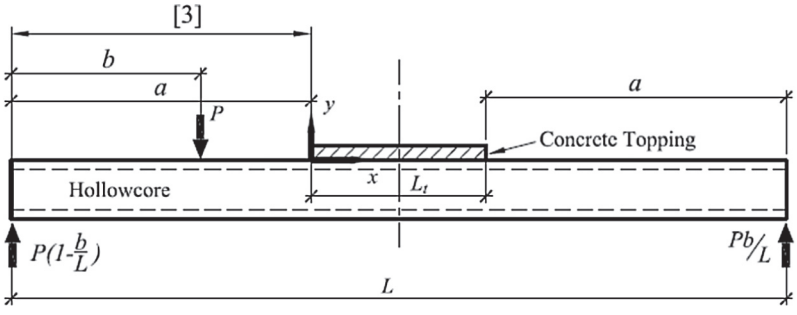

(b) $a > b$

Figure 4 Boundary conditions.

at $x = L_t, M_{hc} = M_T = P\dfrac{ab}{L}$

at $x = (b-a), \tau(x)$ and $\dfrac{d\tau}{dx}(x)$ are continuous functions.

The shear stress is given below for points before and after the concentrated load.

[1] for $0 \leqslant x \leqslant (b-a)$ and $a < b$:

$$\tau(x) = B_3 \cosh(\lambda x) + B_4 \sinh(\lambda x) + m_1 P\left(1 - \frac{b}{L}\right) \quad (14)$$

where $m_2 = \frac{k_s y_{hc}}{E_{hc} I_{hc}}$, $B_3 = \frac{m_2}{\lambda} Pa\left(1 - \frac{b}{L}\right) - m_1 Pe^{-k}$, and $B_4 = \frac{-m_2}{\lambda} Pa\left(1 - \frac{b}{L}\right)$

[2] for $(b-a) \leqslant x \leqslant L_t$ and $a < b$:

$$\tau(x) = B_4 \cosh(\lambda x) + B_5 \sinh(\lambda x) + m_1 P\left(1 - \frac{b}{L}\right) \quad (15)$$

where $B_5 = \frac{m_2}{\lambda} Pa\left(1 - \frac{b}{L}\right) + m_1 P \sinh(k)$ and $B_6 = \frac{-m_2}{\lambda} Pa\left(1 - \frac{b}{L}\right) - m_1 P \sinh(k)$ and $k = \lambda(b-a)$

Case 2: Load acting outside the topping slab ($a > b$), Fig. 4(b):

The boundary conditions for this case are as follows:

at $x = 0, M_T = M_{hc} = Pb\left(1 - \dfrac{a}{L}\right)$

at $x = L_t, M_T = M_{hc} = P\dfrac{ab}{L}$

For any point on the concrete topping, the shear stress will be given by this equation:

$$\tau(x) = B_7 \cosh(\lambda x) + B_8 \sinh(\lambda x) - \left(m_1 P\frac{b}{L}\right) \quad (16)$$

where $B_7 = \frac{m_2}{\lambda} Pb\left(1 - \frac{a}{L}\right)$ and $B_8 = \frac{-m_2}{\lambda} Pb\left(1 - \frac{a}{L}\right)$

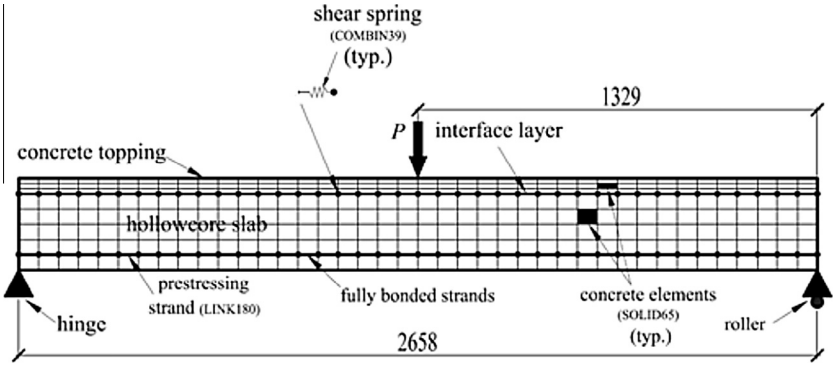

Figure 5 Idealization of the linear FE model.

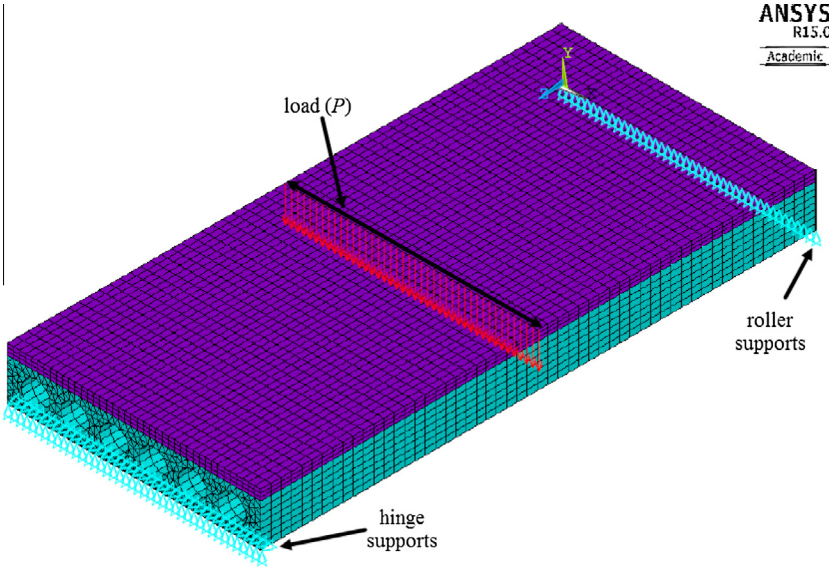

Figure 6 General 3-D view.

4. Linear finite element modeling of the full-scale tests

In this section, a 3-D linear finite element analysis was first performed to check the developed analytical solution. Results were also compared to simplified formulas provided in the North American design standards.

The 3-D FE modeling was conducted using [4]. The full-scale tests were idealized as illustrated in Fig. 5. Element SOLID65 was used to model the hollowcore slab and the concrete topping. LINK180 elements were used to model the prestressing strands. The interfacial shear stiffness between the hollowcore slabs and the topping concrete was modeled using spring elements (COMBIN39).

Values of k_s (interfacial shear stiffness) evaluated by Adawi et al. [2] were utilized. For slabs with machine-cast surface, k_s ranged from 3.48 to 19 (N/mm)/mm^2. The approximate value for k_p was 2.0 (N/mm)/mm^2. A general 3-D view of the loaded slab is given in Fig. 6.

5. Interfacial shear stress distribution

Using the proposed solution given in the previous sections, the shear stress distribution along the interface between the concrete topping and the hollowcore slab was evaluated for the full-scale considered slabs at yielding loads. Two values for (k_s) were used. The resulting distributions are shown in Figs. 7 and 8 for the analytical and finite element modeling.

It can be observed that interfacial shear stress distributions obtained from the proposed analytical solution are comparable with the ones obtained from the linear finite element analysis. This suggests that the proposed analytical solution is adequate, for the studied case. The increase in the interfacial shear stiffness (k_s) slightly increased the maximum shear stress, which occurs at the end section of the studied slabs. This behavior is consistent for both slabs.

The average horizontal shear stress at yielding ($\tau_{avg.}$) was calculated using two methods available in the North American design standards, [6] and ACI 318-08 [1]. The first method depends on the shear force diagram and does not take into account the length of the concrete topping. The second method requires the use of strain compatibility to determine the horizontal shear force in the concrete topping. Table 2 summarizes ($\tau_{avg.}$) along with the maximum shear stress results from the proposed analytical solution and the finite element analysis. The finite element analysis yielded the lowest shear stress values among the three methods shown in the table.

The proposed analytical solution appears to be more consistent with the finite element analysis when used with the upper bound (k_s) value, 19 (N/mm)/mm^2. The methods used in the North American standards appear to be conservative compared to the proposed analytical solution and the finite element analysis, for the studied case.

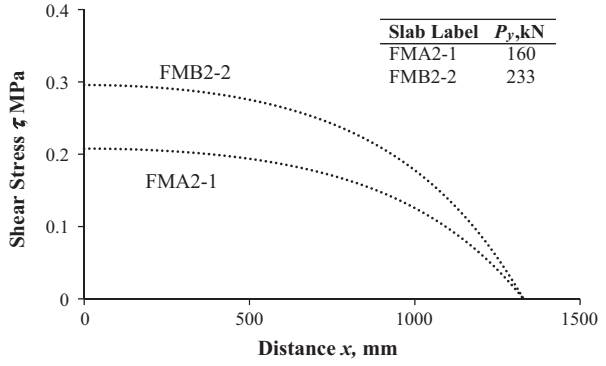

(a) Analytical model.

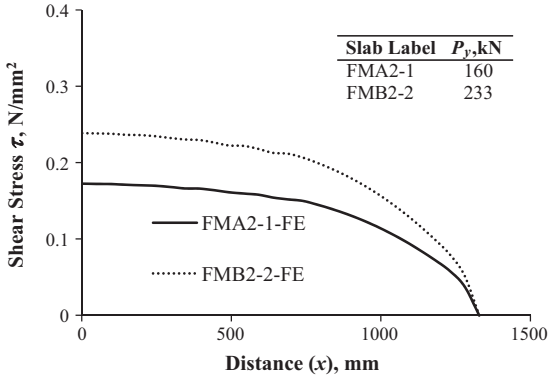

(b) Finite element model.

Figure 7 Shear stress distribution (k_s = 3.48 (N/mm)/mm^2).

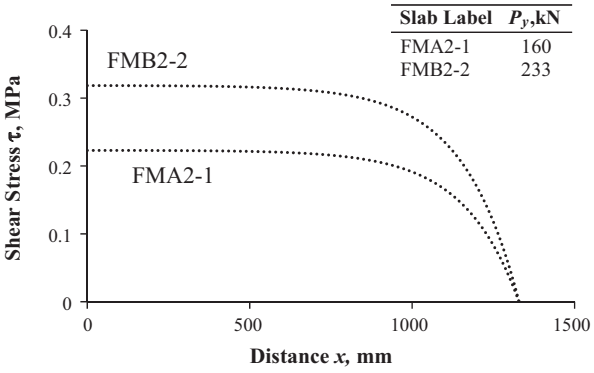

(a) Analytical model.

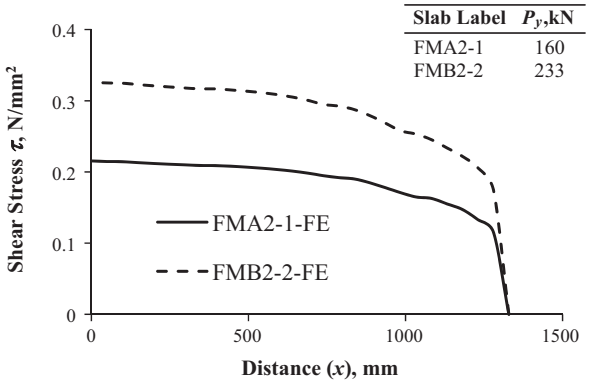

(b) Finite element model.

Figure 8 Shear stress distribution (k_s = 19 (N/mm)/mm^2).

Table 2 Interfacial shear stress results.

Slab Label	Yield load P_y, kN	Max. shear stress τ, MPa				Avg. shear stress (North American Standards), $\tau_{avg.}$ MPa	
		k_s = 3.48 (N/mm)/mm^2		k_s = 19 (N/mm)/mm^2		Method (1)	Method (2)
		Analytical	FE	Analytical	FE		
FMA2-1	160	0.21	0.17	0.22	0.22	0.32	0.34
FMB2-2	233	0.30	0.24	0.32	0.33	0.46	0.50

6. Conclusions

An analytical solution was developed to evaluate the interfacial shear stress distribution along the interface between the concrete topping and the hollowcore slab. For the studied case, the analytical solution seems applicable up to the yielding load level where the composite slab is behaving in the linear elastic zone. In addition, the average interfacial shear stress levels obtained from methods existing in the North American codes were shown to be higher in comparison with the proposed analytical solutions.

In comparison with linear finite element analysis, for the studied cases, it can be concluded that the proposed analytical solution is adequate in estimating the interfacial shear stresses (τ) in composite hollowcore slabs. The shear stiffness coefficients used in this paper were particular for the studied slabs. However, values for any other slab can be estimated using the procedure explained in Adawi et al. [2] using samples from the slabs being studied.

References

[1] ACI 318, Building code requirements for structural concrete (ACI 318-08) and commentary, American Concrete Institute, Michigan, United States, 2008.

[2] A. Adawi, M.A. Youssef, M. Meshaly, Analytical modeling of the interface between lightly roughened hollowcore slabs and cast-in-place concrete topping, J. Struct. Eng. (ASCE) 141 (4) (2014) 1–9.

[3] A. Adawi, M.A. Youssef, M. Meshaly, Experimental investigation of the composite action between hollowcore slabs with machine-cast finish and concrete topping, Eng. Struct. 91 (2015) 1–15.

[4] ANSYS® Academic Research, Release 15.0, 2013, ANSYS Inc.

[5] J. Brozzetti, Design development of steel-concrete composite bridges in France, J. Constr. Steel Res. 55 (1–3) (2000) 229–243.

[6] CSA A23.3, Design of Concrete Structures (A23.3-04), Canadian Standard Association (CSA), Mississauga, ON, Canada, 2004.

[7] B. Jurkiewiez, Static and cyclic behaviour of a steel-concrete composite beam with horizontal shear connections, J. Constr. Steel Res. 65 (12) (2009) 2207–2216.

[8] Q.Q. Liang, B. Uy, M.A. Bradford, H.R. Ronagh, Strength analysis of steel-concrete composite beams in combined bending and shear, J. Struct. Eng. 131 (10) (2005) 1593–1600.

[9] Y. Luo, A. Li, Z. Kang, Parametric study of bonded steel–concrete composite beams by using finite element analysis, Eng. Struct. 34 (2012) 40–51.

[10] J. Nie, Y. Xiao, L. Chen, Experimental studies on shear strength of steel-concrete composite beams, J. Struct. Eng. 130 (8) (2004) 1206–1213.

[11] J.G. Ollgard, R.G. Slutter, J.W. Fischer, Shear strength of stud connectors in lightweight and normal concrete, AISC Eng. J. 8 (1971) 55–64.

[12] F.D. Queiroz, P.C.G.S. Vellasco, D.A. Nethercot, Finite element modeling of composite beams with full and partial shear connection, J. Constr. Steel Res. 63 (2007) (2007) 505–521.

[13] M.R. Salari, E. Spacone, P. Benson, D.M. Frangopol, Nonlinear analysis of composite beams with deformable shear connectors, J. Struct. Eng. (ASCE) (1998) 1148–1158, October.

[14] S.T. Smith, J.G. Teng, Interfacial stresses in plated beams, Eng. Struct. 23 (7) (2001) 857–871.

[15] O. Vilnay, The analysis of reinforced concrete beams strengthened by epoxy bonded steel plates, Int. J. Cem. Compos Lightweight Concr. 10 (2) (1988) 73–78.